Journal of Geography and Geology; Vol. 7, No. 4; 2015
ISSN 1916-9779 E-ISSN 1916-9787
Published by Canadian Center of Science and Education

Analytic Signal and Euler Depth Interpretation of Magnetic Anomalies: Applicability to the Beatrice Greenstone Belt

Thabisani Ndlovu[1], Mashingaidze R. T.[2] & Mpofu P.[3]

[1] Chinhoyi University of Technology, Zimbabwe

[2] National University of Science and Technology, Zimbabwe

[3] Geophysics GPR International, Zimbabwe

Correspondence: Thabisani Ndlovu., Chinhoyi University of Technology, Private Bag 7724, Chinhoyi, Zimbabwe. E-mail: alvin.thabisani@gmail.com

Received: June 18, 2015 Accepted: August 14, 2015 Online Published: November 30, 2015
doi:10.5539/jgg.v7n4p108 URL: http://dx.doi.org/10.5539/jgg.v7n4p108

Abstract

We apply the Analytic Signal and Euler depth filtering techniques on magnetic data to identify a magnetic causative body location-depth relationship, two parameters of importance in both geophysical exploration and ore body modelling. We identify a dipping magnetic contact from the interpreted Euler depth anomalies, showing a good agreement with both the Total Field Magnetic (TFM) map and the Analytic Signal (AS) map. The Euler depth anomalies correlate well with the locations and edges of shallow causative bodies. The deeper Euler interpreted sources explain the magnetic high on the regional aeromagnetic map which is coincident with neither geological contacts nor the more recent dolerite intrusions. This suggests that the magnetic highs on the regional aeromagnetic map are due to deep seated sources, otherwise invisible on the regional geological map. The results show the usefulness and relevancy of these two filters not only in interpreting routine TFM data from the study area, but up to a regional scale. While the aeromagnetic data shows that the magnetisation pattern is predominantly divorced from the geological map, the ground magnetic data interpretation points to a more recent magnetisation of the belt, enabling conclusions to be drawn about the geological history and structural geology otherwise not evident on the geological map.

Keywords: analytic signal, total magnetic field, Euler depth, mineralisation, magnetic anomaly, aeromagnetic map

1. Introduction

The depth and the edges of causative bodies are important parameters, providing information that becomes a guide for the subsequent exploration processes, such as drilling and ore body modeling. The total field magnetic data is usually the first data set to be collected in geophysical exploration (Ghosh, Gupta, Khanna and Singh, 2012). It helps to identify important targets that may need further investigation and the general structural geology. Proper filtering techniques become crucial if much information is to drawn from this preliminary dataset to guide the subsequent exploration processes. It is in this background that the AS and Euler Depth filters are applied to the TFM and interpreted both with respect to each other and the TFM.

Both the analytic signal and Euler depth filtering techniques are normally applied in magnetic data analysis, but interpreted with reference to the total field magnetic map (Ndougsa-Mbarga *et al*., 2012). In this study we focus not only on interpreting the two with reference to the total field magnetic map, but also to each other, highlighting any important correlations in the results from the two techniques. Any similarities between the two filtering techniques will go a long way in validating future magnetic data interpretations within the greenstone belt, allowing rapid deductions to be made.

2. Study Area

The Beatrice greenstone belt is located in the province of Mashonaland East, Zimbabwe at 18°16′S and 30°52′E. It is located about 50 km South-West of Harare on the main Harare- Masvingo road, next to the Umfuri River, a tributary of the Sanyati River in the Zambezi Basin.

The area is at an altitude of between 1320 m and 1450 m above sea level and the topography is generally flat and featureless, except for a few shallow streams and swamps scattered within the study area. Tall and thick grass, scattered thick undergrowth and sandy soils characterize the area. The belt system has previously been explored only at reconnaissance level. According to the Zimbabwe Geological Survey (ZGS) published data, the study area is listed under reconnaissance.

3. Geological Setting

A comparison of the aeromagnetic data and geological maps on Figure 1.1 shows that the aeromagnetic data has no marked visible magnetic signature from the Beatrice Greenstone Belt. The observed magnetic highs are on geological contacts and near some dolerite intrusions. Other magnetic highs are generally not coincident with the borders of the greenstone belt, suggesting that they could be due to deep seated geological sources. The intrusive younger dolerites stated by (Maarten and Lewis, 1997) can be seen on the geological map, with an ultramafic lava intrusion on the south-western edge of the belt. The dominant stratigraphy is of the Bulawayan type, composed of andesitic and dacitic meta-volcanics, is also clear on the geological map, albeit with no magnetic signature on the aeromagnetic map.

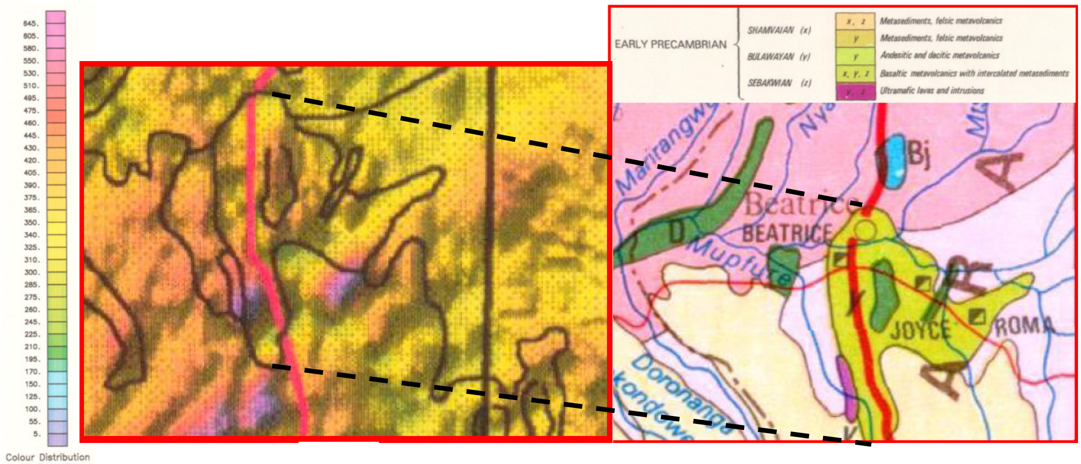

(a) (b)

Figure 1.1 (a) [1]Aeromagnetic and (b) geological Maps of the Beatrice Greenstone Belt

4. Analytic Signal Filtering

The analytic signal can be applied either in space or frequency domain, generating a maximum directly over discrete bodies as well as their edges. Its amplitude is independent on the magnetisation direction. The analytic signal or total gradient is formed through the combination of the horizontal and vertical gradients of the magnetic anomaly (Ansari and Alamdar, 2009). Its form over a causative body depends on the locations of the body (horizontal coordinate and depth) but not on its magnetisation direction. The simplification of magnetic data involves creating a function which is independent of body magnetisation direction and ambient geomagnetic parameters. These parameters are important when remanent magnetization is not negligible. The analytic signal filter possesses this property and has been used for edge detection and depth estimation of magnetic bodies by several authors. Roest *et al* (1992), applied it for detecting causative body location, while Hsu *et al* (1996), used it for geologic boundary edge detection. The filter's ability to generate a maximum value directly over the causative body and depth estimation make it a highly useful technique for magnetic data interpretation (Ansari and Alamdar, 2009)

The amplitude *A* of the analytic signal of the total magnetic field F is calculated from the three orthogonal derivatives of the field, being defined as the square root of the squared sum of the vertical and horizontal derivatives of the magnetic field (Roest *et al*, 1992)

$$|A(x,y)| = \left[\left(\frac{dF}{dx}\right)^2 + \left(\frac{dF}{dy}\right)^2 + \left(\frac{dF}{dz}\right)^2\right]^{1/2} \tag{1}$$

where

A(x, y) is the amplitude of the analytic signal at (x, y), and

F is the observed magnetic field at (x, y)

The derivatives of the gridded map data can be computed in the space domain or in the frequency domain. In our study, the vertical derivative is calculated in the frequency domain and the horizontal derivatives are calculated in the space domain by a finite-difference operator. The amplitude of the analytic signal of the model grid is calculated by applying finite differences to the total magnetic field anomaly computed from the formulas of Singh and Sabina (1978). The horizontal derivatives are calculated directly from a total magnetic field grid using a simple 3x3 filter, while the vertical gradient is calculated using a fast Fourier Transform technique (MacLeod et al.).

The advantage of this magnetic data enhancement method is that its amplitude function is always positive and does not need any assumption of the direction of body magnetization (Jeng *et al*, 2003). In a manner identical to that used in the horizontal gradient method, peaks in the analytic signal amplitude are located**.** The maxima of the analytic signal can be used to detect the structures responsible for the observed magnetic anomalies over the studied area.

5. Euler Depth Method

Euler deconvolution is both a boundary finder and depth estimation method. Euler deconvolution is commonly employed in magnetic interpretation because it requires only a little prior knowledge about the magnetic source geometry, and more importantly, it requires no information about the magnetization vector (Thompson, 1982; Reid *et al*, 1990). Euler deconvolution is based on solving Euler's homogeneity equation (2) (Reid et al., 1990): The rate of field change with distance, applied to map gridded data, can be used to estimate the depth and location of a source by solving Euler's Homogeneity Equation which states that

$$(x - x_0)\frac{dF}{dx} + (y - y_0)\frac{dF}{dx} + (z - z_0)\frac{dF}{dx} = N(B - F) \qquad (2)$$

where x_0, y_0 and z_0 are the source locations whose magnetic field is F, measured at x, y and z, B is the regional value of the total magnetic field, N is the Structural Index (SI) which characterises the source geometry, The most critical parameter in the Euler deconvolution is the structural index, N (Thompson, 1982). This is a homogeneity factor relating the magnetic field and its gradient components to the location of the source. Essentially, N measures the rate of change of the fields with distance from the source (fall-off-rate) and is directly related to the source dimensions. Therefore, by changing N, we can estimate the geometry and depth of the magnetic sources. A poor choice of the structural index has been shown to cause a diffuse solution of source locations and serious biases in depth estimation. Both Thompson (1982) and Reid et al (1990) suggested that a correct N gives the tightest clustering of the Euler solutions around the geologic structure of interest. For magnetic data, physically plausible N values range from 0 to 3 taking the values of zero (for contact of infinite depth extent), 0,5 (for linear basement of dyke), 1(for thin dyke), 2 (for pipe) and 3 for spherical bodies (Ghosh et al, 2012).

6. Data Collection and Processing

The 0,6 km² area was divided into 20 parallel lines in the direction south-east to north-west, with a line spacing of 50 m and a station spacing of 10 m, using an e-Trex Geographical Positioning

System (GPS) .The magnetic data was collected using three GSM 19 Overhauser Magnetometers. One magnetometer was used at the base station, located at a magnetically quiet site. The reference datum was chosen to be 30383 nT. The Overhauser Magnetometer has a magnetic resolution of 0.1 nT and a non-volatile CMOS memory and a capacity of 15000 readings. The base station magnetometer was programmed to take readings at an interval of 30 s. The two roving survey teams where assigned Team A and Team B, starting at line 0 and line 550 respectively. Each team incremented their survey lines from their start position. The roving units took readings every 10 m, making a total of 60 readings per line and 1100 readings in two days. The Day 1 survey covering 10 lines (0 -300) and lines 550-850. The ensuring overnight interpretation showed that lines 900-1000 had no anomaly; hence Day 2 was dedicated to lines 350 -500. The data was dumped onto a personal computer using the GEMLinkW 4.0 Ink software system and processed using the Geosoft Oasis Montaj software.

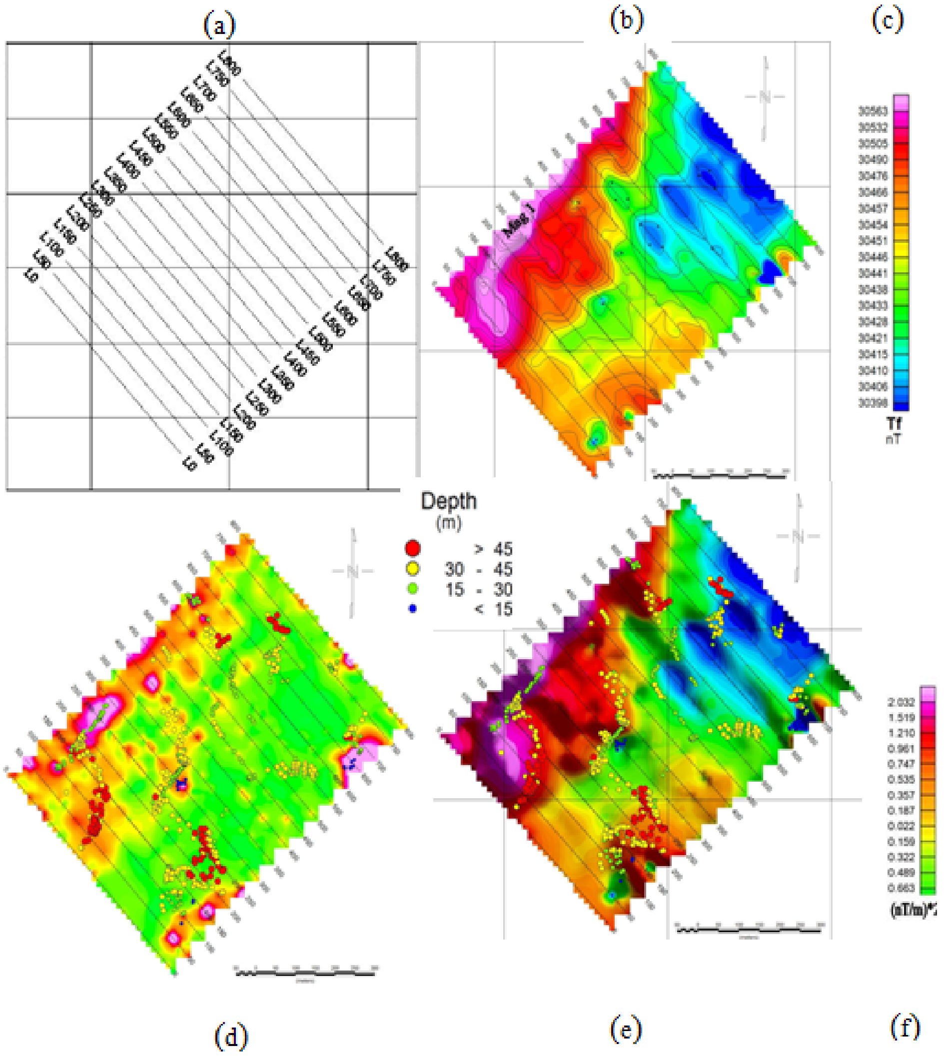

Figure 1.2 (a) Survey Area Grid, (b) TFM Map, (c) TFM Map legend, (d) AS Map with Euler Depth interpretation, (e) Sun-shaded TFM with Euler Depth Interpretation and (f) AS Map Legend

7. Results and Interpretation

There is a 170 nT gradation in the TFM magnetic readings, with the highest magnetic readings on the north-western part of the grid, magnetic anomaly Mag 1 .The anomaly has a NE-SW strike and has an average thickness of 70 m. The analytic signal and Euler depth map show that most of the magnetic anomalies coincide with the interpreted shallow sources. The analytic signal generates a maximum directly over discrete bodies as well as their edges, and thus the AS anomalies are mark the edges and tops of the TFM anomalies. The arrangement of the Euler depth markers around the magnetic high generally shows a change from shallower to deeper as you move south away from Mag 1.

8. Conclusion

The interpreted Euler depths coincide with AS anomalies, especially on the edges of the Mag 1 anomaly. This enables us to identify the depth-location of the causative body. Interpreting these anomalies with respect to the TFM map enables us not only to locate the causative body location, but its dip direction and likely shape at that depth. The coincidence of AS anomalies and Euler depths implies that the edges of the magnetic body have been properly resolved by the filters. The interpretation is thus valid both on the edges and top of the Mag 1 anomaly. The Euler interpretation further highlights some deep seated magnetic sources, and these can be used to explain the aeromagnetic highs that are not coincident with the structural edges on the geological map of the study area. The magnetic properties of the study area are thus not guided by the geological map, and this is in agreement with the aeromagnetic map results.

A change from shallower to deeper sources is observed as you move south, away from the Mag 1 anomaly, suggesting that the magnetic contact is dipping towards the south. We conclude that the AS and Euler depth interpretation techniques are applicable for the processing of magnetic data in the study area, enabling conclusions to be drawn about the structural geology otherwise not evident on the geological map.

Acknowledgements

The authors wish to acknowledge the equipment and resource support by Geophysics GPR international and the Geological Survey of Zimbabwe.

References

Ansari, A. H., & Alamdar, K. (2009). Reduction to the Pole of Magnetic Anomalies Using Analytic Signal. *World Applied Sciences Journal, 7*(4), 405-409. ISSN 1818-4952.

Bartholomew, D. S. (1990). Gold Deposits of Zimbabwe: *Mineral Resources Series #23*; *ZGS*, Harare, 1990, p18, 23, 26.

Ghosh, G. K., Gupta, R. D., Khanna, A. K., & Singh, S. N. (2012). Application of Euler Deconvolution of Gravity and Magnetic Data for Basement Depth Estimation in Mizoram Area. *Geohorizons*, 13-19. http://dx.doi.org/10.3997/2214-4609.20143715

Hsu, S. K., Sibuet, J. C., & Shyu, C. T. (1996). High-resolution detection of geologic boundaries from potential-field anomalies; an enhanced analytic signal technique**.** *Geophysics, 61*, 373-386. http://dx.doi.org/10.1190/1.1443966

Jeng, Y., Lee, Y. L., Chen, C. Y., & Lin, M. J. (2003). Integrated signal enhancements in magnetic investigation in archaeology. *Journal of Applied Geophysics, 53*, 31–48. http://dx.doi.org/10.1016/S0926-9851(03)00015-6

Kirkpatric, I. M. (1968). Dolerite intrusions of the Beatrice area*. Unpublished ZGS Technical Report.* B10/20, 5

Maarten, J. D. W., & Lewis, D. A. (1997). Greenstone Belts*. Clarendon Press*, 37-47. *Mining Coordinating Unit (MCU) of the Southern African Development Community (SADC) and European Commission*. (1994).Report, Lusaka, Zambia.

MacLeod, I. N., Jones, K., & Dai, T. F. (1993). 3-D analytic signal in the interpretation of Total magnetic field data at low magnetic latitudes. *Exploration Geophysics, 24*(4), 679–688. http://dx.doi.org/10.1071/EG993679

Ndougsa-Mbarga, T., Feumo, N. S. A., Manguelle-Dicoum, E., & Fairhead, D. J. (2012). Aeromagnetic Data Interpretation to Locate Buried Faults in South-East Cameroon. *Geophysica, 48*(1–2), 49–63.

Reid, A. B., Allsop, J. M., Granser, H., Millett, A. J., & Somerton, I. W. (1990). Magnetic interpretation in three dimensions using Euler deconvolution. *Geophysics, 55*, 80–90. http://dx.doi.org/10.1190/1.1442774

Roest, W. R., Verhoef, J., & Pilkington, M. (1992). Magnetic interpretation using the 3-D analytic Signal. *Geophysics, 57*(6), 116-125. http://dx.doi.org/10.1190/1.1443174

Sabina, F. J. (1978). Magnetic anomaly due to a vertical right circular cylinder with arbitrary polarization: *Geophysics, 43*, 173–178.

Singh, S. K., & MacLeod, I. N., Jones, K., & Dai, T. F. (1993). 3-D Analytic Signal in the Interpretation of Total Magnetic Field Data at Low Magnetic Latitudes. *Exploration Geophysics, 24*(670-688).

Subasinghe, N., Charles, W., & Silva, S. (2014). Analytical Signal and Reduction to Pole Interpretation of Total Magnetic Field Data at Eppawala Phosphate Deposit. *Journal of Geoscience and Environment Protection, 2*, 181-189. http://dx.doi.org/10.4236/gep.2014.23023

Thompson, D. T. (1982). EULDPH: A new technique for making computer-assisted depth estimates from magnetic data. *Geophysics, 47*, 31–37., http://dx.doi.org/10.1190/1.1441278

Copyrights